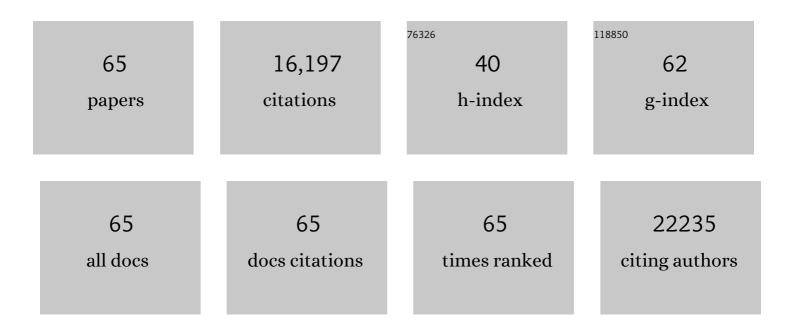
## **Rachid Sougrat**

List of Publications by Year in descending order

Source: https://exaly.com/author-pdf/706298/publications.pdf Version: 2024-02-01



PACHID SOUCPAT

#	Article	IF	CITATIONS
1	Enhanced photocatalytic hydrogen evolution from organic semiconductor heterojunction nanoparticles. Nature Materials, 2020, 19, 559-565.	27.5	366
2	3D Analysis of Ordered Porous Polymeric Particles using Complementary Electron Microscopy Methods. Scientific Reports, 2019, 9, 13987.	3.3	17
3	Cytosolic aggregates in presence of nonâ€ŧranslocated proteins perturb endoplasmic reticulum structure and dynamics. Traffic, 2019, 20, 943-960.	2.7	8
4	Atomic-resolution transmission electron microscopy of electron beam–sensitive crystalline materials. Science, 2018, 359, 675-679.	12.6	374
5	Functionalized Nanochannels from Selfâ€Assembled and Photomodified Poly(Styreneâ€ <i>b</i> â€Butadieneâ€ <i>b</i> â€Styrene). Small, 2018, 14, e1701885.	10.0	19
6	Artificial 3D hierarchical and isotropic porous polymeric materials. Science Advances, 2018, 4, eaat0713.	10.3	31
7	MXenes stretch hydrogel sensor performance to new limits. Science Advances, 2018, 4, eaat0098.	10.3	556
8	Unravelling surface and interfacial structures of a metal–organic framework by transmission electron microscopy. Nature Materials, 2017, 16, 532-536.	27.5	306
9	Not just a marker: CD34 on human hematopoietic stem/progenitor cells dominates vascular selectin binding along with CD44. Blood Advances, 2017, 1, 2799-2816.	5.2	73
10	Synthesis of highly porous poly(tert-butyl acrylate)-b-polysulfone-b-poly(tert-butyl acrylate) asymmetric membranes. Polymer Chemistry, 2016, 7, 3076-3089.	3.9	28
11	3D visualization of the internal nanostructure of polyamide thin films in RO membranes. Journal of Membrane Science, 2016, 501, 33-44.	8.2	149
12	Developments in TEM Nanotomography of Calcium Silicate Hydrate. Journal of the American Ceramic Society, 2015, 98, 2307-2312.	3.8	15
13	Non-chemotoxic induction of cancer cell death using magnetic nanowires. International Journal of Nanomedicine, 2015, 10, 2141.	6.7	90
14	Nanocapsules with fluorous filling: A "molecular zipper―approach. Journal of Polymer Science Part A, 2015, 53, 215-218.	2.3	1
15	Enzyme-Inspired Functional Surfactant for Aerobic Oxidation of Activated Alcohols to Aldehydes in Water. ACS Catalysis, 2015, 5, 1313-1317.	11.2	43
16	Compatibilizing role of carbon nanotubes in poly(vinyl alcohol)/starch blend. Starch/Staerke, 2015, 67, 147-153.	2.1	41
17	Microbial Community Composition and Ultrastructure of Granules from a Full-Scale Anammox Reactor. Microbial Ecology, 2015, 70, 118-131.	2.8	115
18	Ionic liquids as self-assembly guide for the formation of nanostructured block copolymer membranes. Journal of Membrane Science, 2015, 492, 568-577.	8.2	32

RACHID SOUGRAT

#	Article	IF	CITATIONS
19	Synthesis and characterization of polystyrene coated iron oxide nanoparticles and asymmetric assemblies by phase inversion. Journal of Applied Polymer Science, 2015, 132, .	2.6	9
20	Mechanical, Rheological and Thermal Properties of Polystyrene/1-Octadecanol Modified Carbon Nanotubes Nanocomposites. Fullerenes Nanotubes and Carbon Nanostructures, 2015, 23, 209-217.	2.1	9
21	Silver-Enhanced Block Copolymer Membranes with Biocidal Activity. ACS Applied Materials & Interfaces, 2014, 6, 18497-18501.	8.0	58
22	One-Pot Synthesis of Au@SiO <sub>2</sub> Catalysts: A Click Chemistry Approach. ACS Combinatorial Science, 2014, 16, 513-517.	3.8	16
23	Facile synthesis and application of a carbon foam with large mesopores. Physical Chemistry Chemical Physics, 2013, 15, 19134.	2.8	7
24	<i>Batf3</i> and <i>Id2</i> Have a Synergistic Effect on <i>Irf8</i> -Directed Classical CD8α+ Dendritic Cell Development. Journal of Immunology, 2013, 191, 5993-6001.	0.8	37
25	Block Copolymer Hollow Fiber Membranes with Catalytic Activity and pH-Response. ACS Applied Materials & Interfaces, 2013, 5, 7001-7006.	8.0	69
26	Effective antireflection properties of porous silicon nanowires for photovoltaic applications. , 2013, ,		8
27	Hollow Au@Pd and Au@Pt core–shell nanoparticles as electrocatalysts for ethanol oxidation reactions. Journal of Materials Chemistry, 2012, 22, 25003.	6.7	140
28	Successful implementation of the stepwise layer-by-layer growth of MOF thin films on confined surfaces: mesoporous silica foam as a first case study. Chemical Communications, 2012, 48, 11434.	4.1	98
29	Effect of Mn doped-titania on the activity of metallocene catalyst by in situ ethylene polymerization. Journal of Industrial and Engineering Chemistry, 2012, 18, 1836-1840.	5.8	11
30	Zippered release from polymer-gated carbon nanotubes. Journal of Materials Chemistry, 2012, 22, 11503.	6.7	17
31	Solutionâ€Processed Small Moleculeâ€Polymer Blend Organic Thinâ€Film Transistors with Hole Mobility Greater than 5 cm <sup>2</sup> /Vs. Advanced Materials, 2012, 24, 2441-2446.	21.0	219
32	Nanoroses of Nickel Oxides: Synthesis, Electron Tomography Study, and Application in CO Oxidation and Energy Storage. ChemSusChem, 2012, 5, 1241-1248.	6.8	30
33	Nanoblock Aggregationâ^'Disaggregation of Zeolite Nanoparticles: Temperature Control on Crystallinity. Journal of Physical Chemistry C, 2011, 115, 7285-7291.	3.1	9
34	From Micelle Supramolecular Assemblies in Selective Solvents to Isoporous Membranes. Langmuir, 2011, 27, 10184-10190.	3.5	99
35	Switchable pH-Responsive Polymeric Membranes Prepared <i>via</i> Block Copolymer Micelle Assembly. ACS Nano, 2011, 5, 3516-3522.	14.6	255
36	A role for actin arcs in the leading-edge advance of migrating cells. Nature Cell Biology, 2011, 13, 371-382.	10.3	314

RACHID SOUGRAT

#	Article	IF	CITATIONS
37	The Glycolytic Shift in Fumarate-Hydratase-Deficient Kidney Cancer Lowers AMPK Levels, Increases Anabolic Propensities and Lowers Cellular Iron Levels. Cancer Cell, 2011, 20, 315-327.	16.8	190
38	Effect of acid treated carbon nanotubes on mechanical, rheological and thermal properties of polystyrene nanocomposites. Composites Part B: Engineering, 2011, 42, 1554-1561.	12.0	79
39	Dynamics of endosomal sorting complex required for transport (ESCRT) machinery during cytokinesis and its role in abscission. Proceedings of the National Academy of Sciences of the United States of America, 2011, 108, 4846-4851.	7.1	346
40	The effect of butenolide on behavioral and morphological changes in two marine fouling species, the barnacle <i>Balanus amphitrite</i> and the bryozoan <i>Bugula neritina</i> . Biofouling, 2011, 27, 467-475.	2.2	17
41	Interaction between the Triglyceride Lipase ATGL and the Arf1 Activator GBF1. PLoS ONE, 2011, 6, e21889.	2.5	56
42	Iron Insufficiency Compromises Motor Neurons and Their Mitochondrial Function in Irp2-Null Mice. PLoS ONE, 2011, 6, e25404.	2.5	49
43	Three-Dimensional Scanning Transmission Electron Microscopy of Biological Specimens. Microscopy and Microanalysis, 2010, 16, 54-63.	0.4	45
44	Serum ferritin is derived primarily from macrophages through a nonclassical secretory pathway. Blood, 2010, 116, 1574-1584.	1.4	364
45	Multilayered Mechanism of CD4 Downregulation by HIV-1 Vpu Involving Distinct ER Retention and ERAD Targeting Steps. PLoS Pathogens, 2010, 6, e1000869.	4.7	145
46	Mitochondria Supply Membranes for Autophagosome Biogenesis during Starvation. Cell, 2010, 141, 656-667.	28.9	1,200
47	Ultraporous Films with Uniform Nanochannels by Block Copolymer Micelles Assembly. Macromolecules, 2010, 43, 8079-8085.	4.8	200
48	Human Immunodeficiency Virus Type 1 Nef Protein Targets CD4 to the Multivesicular Body Pathway. Journal of Virology, 2009, 83, 6578-6590.	3.4	57
49	Phoenix Is Required for Mechanosensory Hair Cell Regeneration in the Zebrafish Lateral Line. PLoS Genetics, 2009, 5, e1000455.	3.5	67
50	Coatomer-dependent protein delivery to lipid droplets. Journal of Cell Science, 2009, 122, 1834-1841.	2.0	216
51	Molecular investigations to improve diagnostic accuracy in patients with ARC syndrome. Human Mutation, 2009, 30, E330-E337.	2.5	40
52	Interferometric fluorescent super-resolution microscopy resolves 3D cellular ultrastructure. Proceedings of the National Academy of Sciences of the United States of America, 2009, 106, 3125-3130.	7.1	816
53	Electron tomography of the Maurer's cleft organelles of <i>Plasmodium falciparum</i> â€infected erythrocytes reveals novel structural features. Molecular Microbiology, 2008, 67, 703-718.	2.5	80
54	The Twists and Turns of Maurer's Cleft Trafficking in <i>P. falciparum</i> â€Infected Erythrocytes. Traffic, 2008, 9, 187-197.	2.7	64

**RACHID SOUGRAT** 

#	ARTICLE	IF	CITATIONS
55	Electron Tomography of the Contact between T Cells and SIV/HIV-1: Implications for Viral Entry. PLoS Pathogens, 2007, 3, e63.	4.7	165
56	Analysis of De Novo Golgi Complex Formation after Enzyme-based Inactivation. Molecular Biology of the Cell, 2007, 18, 4637-4647.	2.1	17
57	Gigabytes to Bytes: Automated Denoising and Feature Extraction as Applied to the Analysis of HIV Architecture and Variability using Electron Tomography. , 2007, , .		0
58	Electron tomography of viruses. Current Opinion in Structural Biology, 2007, 17, 596-602.	5.7	54
59	Imaging Intracellular Fluorescent Proteins at Nanometer Resolution. Science, 2006, 313, 1642-1645.	12.6	7,580
60	Golgi Inheritance in Mammalian Cells Is Mediated through Endoplasmic Reticulum Export Activities. Molecular Biology of the Cell, 2006, 17, 990-1005.	2.1	108
61	Golgi Inheritance Under a Block of Anterograde and Retrograde Traffic. Traffic, 2004, 5, 284-299.	2.7	11
62	Molecular basis for Golgi maintenance and biogenesis. Current Opinion in Cell Biology, 2004, 16, 364-372.	5.4	144
63	Impaired Stratum Corneum Hydration in Mice Lacking Epidermal Water Channel Aquaporin-3. Journal of Biological Chemistry, 2002, 277, 17147-17153.	3.4	236
64	Functional Expression of AQP3 in Human Skin Epidermis and Reconstructed Epidermis. Journal of Investigative Dermatology, 2002, 118, 678-685.	0.7	172
65	Effect of High Shear Mixing Parameters and Degassing Temperature on the Morphology of Epoxy-Clay Nanocomposites. Advanced Materials Research, 0, 652-654, 159-166.	0.3	10